Journal of Magnetic Resonance 301 (2019) 30–39

Contents lists available at ScienceDirect

Journal of Magnetic Resonance

journal homepage: www.elsevier.com/locate/jmr

Optimizing the transformation of HYSCORE data using the maximum entropy algorithm

Alina E. Motygullina, Mehdi Mobli, Jeffrey R. Harmer *

The Centre for Advanced Imaging, University of Queensland, St Lucia, QLD 4072, Australia

ARTICLE INFO

Article history:
Received 18 January 2019
Revised 20 February 2019
Accepted 21 February 2019
Available online 23 February 2019

Keywords:
EPR
HYSCORE
Non-uniform sampling
Maximum entropy algorithm

ABSTRACT

Non-uniform sampling (NUS) in combination with the Maximum Entropy (MaxEnt) algorithm as applied to multi-dimensional NMR data has been thoroughly investigated and the NUS approach shown to provide significant sensitivity improvements as compared to methods using uniformly sampled (US) data and the discrete Fourier transform (DFT). Hyperfine sublevel correlation (HYSCORE) is a standard pulse EPR experiment that can potentially benefit greatly from this approach, but the data present unique challenges as compared to NMR. HYSCORE data typically exhibit a very large range of peak intensities, signals are in the form of irregularly shaped ridges with variable intensities, and time traces are generally truncated to save measurement time. MaxEnt has the advantageous properties that it does not require US data, dampens weak signals (noise) and does not suffer from windowing artifacts due to truncation of the time traces. Critical to the success of the MaxEnt algorithm is the choice of the two input parameters *aim* and *def* which describe the data noise and contribution of entropy in the optimization, respectively. In this paper we expand our preliminary study on the application of MaxEnt to the reconstruction of HYSCORE spectra to include a detailed analysis on sensitivity to detect weak peaks, investigate the non-linearity of the transformation and ascertain if it can be characterized by the introduction of synthetic peaks, and define a general range for the choice of *aim* and *def*. Furthermore, the ability of the MaxEnt method to remove windowing artefacts in uniformly sampled truncated HYSCORE data is described.

1. Introduction

Pulse electron paramagnetic resonance (EPR) offers the possibility to characterize paramagnetic systems in great detail by allowing many of the unresolved couplings in a continuous wave (CW) EPR spectrum to be resolved and quantified. Time-domain pulse EPR experiments [1] are typically carried out by recording the intensity of an electron-spin echo while incrementing one or more delays in the pulse sequence. A discrete Fourier transformation (FT) is then almost universally used to compute the frequency domain spectrum from which the magnetic couplings can be conveniently extracted, often via simulation [2]. The most widely used and informative electron spin echo envelope (ESEEM) experiment to measure hyperfine and nuclear quadrupole couplings uses the four pulse hyperfine sublevel correlation (HYSCORE) sequence [1,3]. Even though EPR experiments are in general considered sensitive due to the large electron spin magnetic moment, the time required to record data from multi-dimensional pulse EPR experiments with two or more indirect dimensions is often prohibitive. This is particularly relevant for paramagnetic centers in biological samples which may only be available at low concentrations (e.g. < 10 μM), and also for minor species in multi-component mixtures. To overcome sensitivity issues, the time trace length can be reduced, albeit at the expense of resolution, or as we showed in a preliminary report [4], the time domain data can be sampled non-uniformly and the frequency spectrum reconstructed using the method of Maximum Entropy (MaxEnt).

In this paper we will again concentrate on the two-dimensional (2D) technique HYSCORE. The sequence (Fig. 1) has two indirect dimensions, with both t_1 and t_2 requiring stepwise incrementation to record a matrix of intensities in the time domain, $\mathbf{Y}(t_1,t_2)$. This incrementation scheme makes the data measurement time consuming, and as a result HYSCORE data is often truncated before signals have decayed to below the noise level.

In multi-dimensional NMR spectroscopy, non-uniform sampling (NUS) schemes in conjunction with the method of Maximum Entropy (MaxEnt) for spectrum reconstruction have been intensely investigated over the last decades [5–15]. The main advantage of this methodology for NMR data is a significant reduction in

* Corresponding author.
E-mail address: jeffrey.harmer@cai.uq.edu.au (J.R. Harmer).

https://doi.org/10.1016/j.jmr.2019.02.002
1090-7807/

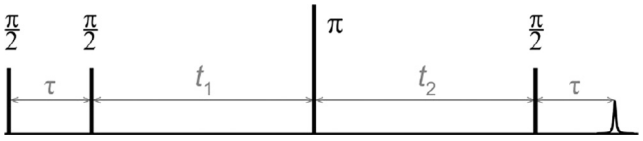

Fig. 1. Hyperfine sublevel correlation (HYSCORE) pulse sequence, the time-domain matrix is collected as $\mathbf{Y}(t_1, t_2)$ for a fixed τ. The experiment correlates nuclear frequencies in the different electron spin manifolds, yielding cross-peaks symmetric to the diagonals in the frequency domain spectrum, the frequencies of which are determined by electron-nuclear interactions (e.g. nuclear Zeeman, hyperfine and nuclear quadrupole) [1].

measurement time with an increase in resolution [8]. In NMR spectroscopy the NUS + MaxEnt methodology is developing into a key technique because of a number of desirable properties: (1) it is free of prejudice concerning missing data points in a NUS scheme, (2) it does not exhibit 'starred peaks' or 'sinc-wiggle' artefacts as the frequency domain is determined directly, and (3) artifact signals in the reconstructed spectrum are minimized due to the incorporation of an entropy term into the objective function.

A disadvantage of the MaxEnt algorithm is that it scales signal intensity and thus peaks non-linearly by pushing weaker intensities more toward zero as compared to stronger intensities [16,17]. Consequently, it is unlikely that noise will be falsely identified as peaks in a well optimized MaxEnt spectrum, but the weakest real peaks could be lost in the noise, leading potentially to a loss of information. The exact details of the MaxEnt spectrum reconstruction depends upon two user input variables *aim* and *def*. The goodness of fit is defined by *aim* and is best adjusted in accordance with the noise level of the data, and *def* controls the relative weighting of the entropy term in the objective function and is chosen relative to *aim*. These two parameters dictate the degree of non-linearity of the reconstruction of the spectrum intensities. The non-linear characteristic of the MaxEnt algorithm makes accurate quantification of peak heights in general difficult. To be reliable for HYSCORE applications, the dependence of the MaxEnt parameters on the optimized spectrum needs to be well understood and characterized.

Although the nature of the data to be transformed by HYSCORE and *n*-dimensional NMR is in principle similar, the techniques have large differences in the details of the spectrum, with HYSCORE spectra typically exhibiting long ridges of irregular shape with variable linewidths, and peak intensities which very often vary by an order of magnitude or more [4]. Therefore, if the NUS + MaxEnt method is to be employed generally to HYSCORE data, the user adjustable parameters of the algorithm should be investigated and suitable ranges defined for the specific requirements of HYSCORE. In our preliminary paper on the application of the MaxEnt algorithm to HYSCORE data, we investigated non-uniform sampling (NUS) schemes and determined that about 20% or less of the linearly sampled data points were required to accurately compute a spectrum where the peak positions (frequencies) are faithfully determined [4]. This established that significant reductions in measurement times are possible with minimal distortions of the frequency spectrum in terms of peak positions. However, we did not investigate in any detail the sensitivity with respect to detection of the weakest peaks, the non-linearity of the frequency spectrum reconstruction, or the shape of the HYSCORE ridges and peaks. These aspects therefore warrant a detailed study.

In this paper we explore the use of the maximum entropy approach and its dependence on *aim* and *def* in terms of (1) sensitivity to detect the weakest peaks in the spectrum, (2) ability to faithfully reconstruct the shape of HYSCORE ridges, and (3) on the non-linearity of the reconstruction and if it can be characterized by the introduction of synthetic peaks with known intensities. To characterize sensitivity to detect the weakest peaks two datasets are utilized; one where only one set of cross-peaks is detected with a poor signal-to-noise ratio (SNR) and poor spectral resolution, and a second where many cross-peaks are observed with a large range of signal intensities and with high spectral resolution. The sensitivity for constant time experiments and minimum time experiments for both US + DFT and NUS + MaxEnt are explored. MaxEnt sensitivity, linearity and shape of HYSCORE ridges on *aim* and *def* are characterized. Lastly, we show how the MaxEnt algorithm applied to linearly sampled data can be used as an alternative to the routinely employed DFT that suffers from windowing artifacts. This approach was already investigated in 1995 by Hore [18] in relation to NMR data processing, but is potentially more relevant to HYSCORE data as normally the time domain data is truncated which results in starred peaks ("sinc wiggles") in the frequency domain, a problem exacerbated by peak intensities which vary by more than an order of magnitude. This characteristic makes the weakest peaks susceptible to distortions from windowing artifacts from the strongest peaks.

2. Methods

2.1. MaxEnt algorithm for spectral reconstruction

Here we provide an overview of aspects of MaxEnt that are important for this work, in particular HYSCORE. A detailed overview of the MaxEnt reconstruction method for NMR spectra is discussed in detail elsewhere [6,18–22]. The MaxEnt reconstruction of HYSCORE data was carried out using the Rowland NMR Toolkit (RNMRTK) [23–25] which finds the spectrum $\boldsymbol{f}$ which maximizes the entropy $S(\boldsymbol{f})$, and which at the same time is consistent with the experimental (measured) data $\mathbf{d}$. The MaxEnt objective function $Q(\mathbf{f}, \mathbf{d})$ to be maximized is,

$$Q(\boldsymbol{f}, \boldsymbol{d}) = S(\boldsymbol{f}) - \lambda C(\boldsymbol{f}, \boldsymbol{d}), \tag{1}$$

where λ is a Lagrange multiplier that determines the relative weight of the entropy contribution to the objective function. The term C($\mathbf{f}$, $\mathbf{d}$) quantifies the fit of the frequency domain reconstruction to the time-domain experimental data,

$$C(\mathbf{f}, \mathbf{d}) = \sum_{i=1}^{N} |m_i - d_i|^2 = \sum_{i=1}^{N} \left|IDFT(\boldsymbol{f})_i - d_i\right|^2 \leqslant C_0 \equiv aim, \tag{2}$$

where m_i is the reconstructed time domain data, computed from the inverse Fourier transform of $\mathbf{f}$. Experimental data $\mathbf{d}$ has N elements d_i. The spectrum $\boldsymbol{f}$ is considered to be consistent with $\mathbf{d}$ when $C(\mathbf{f},\mathbf{d}) \leq C_0$, where C_0 is typically chosen in relation to the experimental noise (as discussed later a good value for HYSCORE is in the range 0.5 – 0.1 of the data noise level value). Usually in the literature C_0 is referred to as *aim*, and for the sake of clarity, we will also refer to *aim* instead of C_0. For a complex phase-sensitive spectrum, the entropy can be defined as,

$$S(\boldsymbol{f}) = -\sum_{n=0}^{N-1} \frac{|f_n|}{def} \log\left(\left(|f_n|/def + \sqrt{4 + |f_n|^2/def^2}\right)/2\right) - \sqrt{4 + |f_n|^2/def^2} \tag{3}$$

where *def* is a scale factor that can be interpreted as a default value which function $\mathbf{f}$ would attain in the absence of experimental signals (i.e. the data only contains noise) [20]. It can be shown that the *def* value can be defined from a quantum-mechanical derivation [6], but it is more applicable for this application to treat *def* as a user adjustable parameter and note that its value influences the non-linearity of the frequency domain reconstruction. In the case of HYSCORE the absolute value of the frequency domain data is used and thus the conventional Shannon entropy could also be used,

$$S(\boldsymbol{f}) = -\sum_{n=0}^{N-1} \frac{|f_n|}{def} \ln\left(\frac{|f_n|}{def}\right). \quad (4)$$

Daniell and co-workers [21] compared the usage of both functions (3) and (4), and showed their similarity for positive real frequency data. In this paper Eq. (3) is used. For completeness we note that for phase-sensitive NMR data the entropy representation should take the form of Eq. (3), see Ref. [21] for details.

There are two essentially equivalent optimization options for the RNMRTK MaxEnt algorithm: "constant λ" regime with *aim* adjusted during algorithm convergence, or "constant *aim*" regime with λ adjusted during algorithm convergence [6,17]. Both approaches should in principle produce an essentially equivalent result as the convergence criteria are identical. The advantage of one approach over the other is discussed in detail in Ref. [17]; for quantification purposes (obtaining a fit relative to the noise level) the "constant *aim*" approach is generally the most reliable and is used in our work. Setting *aim* to a very small number results in the reconstructed time-domain data **m** fitting very accurately to the experimental data **d**, which in the extreme case results in the MaxEnt spectrum being fitted also to the noise.

2.2. Defining aim from the data noise level

To define an *aim* value the noise level of the spectrum is required. In NMR, this can be conveniently achieved using the root mean square (RMS) deviation of the data at the end of the FIDs in the direct dimension where the signals have essentially decayed to zero and only noise remains. Since both dimension in HYSCORE are indirect, this can be problematic as the time traces are invariably truncated in both dimensions. A simple approach is to carry out a second short experiment where only one HYSCORE trace is recorded for a time sufficient that the signal, the ESEEMs, have decayed to zero. We used this approach in this work. A second approach is to calculate noise in the frequency-domain at a signal-free area and convert this to time-domain noise [22] using Parseval's theorem. In this paper both methods were trialed and give essential the same value for *aim* in all cases. Note that the frequency-domain option is not sensible if only NUS time-domain data is available as a FT in this case is not reliable. In a third elegant approach noise can be analyzed in the time domain from a set of individual scans which circumvents the need to remove the baseline as described in the supporting information of Ref. [26].

2.3. Experimental

HYSCORE spectra were recorded with the four pulse sequence shown in Fig. 1. A 4-step phase cycle was used to remove unwanted echoes [1]. Three X-band HYSCORE datasets at 15 K were collected for analysis, all on a P450 enzyme (ca. 400 μM loaded into an OD 3.8 mm quartz EPR tube) at an observer position close to the g_2 position in the middle of its frozen-solution CW EPR spectrum ($B_0 \approx 310$ mT, microwave frequency ≈9.748 GHz). Peak assignments are given in Fig. S1 for completeness. All experiments had pulse lengths of $t_\pi = 16$ ns, $t_{\pi/2} = 16$ ns, and both t_1 and t_2 times start at $t_0 = 32$ ns. The individual datasets used the following parameters. Dataset-1: 125×125 points, time increments $\Delta t = 20$ ns (Nyquist frequency 2×25 MHz, t_1, $t_2 = 2480$ ns), repetition time 0.7 ms, total acquisition time ca. 4 min. A total of 40 individual HYSCORE data matrices were recorded, each is referred to as 1 accumulation. Dataset-1 exhibits a very low signal-to-noise ratio (SNR). Dataset-2: 400×400 points, time increments $\Delta t = 18$ ns (Nyquist frequency 2×27.78 MHz, t_1, $t_2 = 7182$ ns), repetition time 1 ms, total acquisition time ca. 11 min. A total of 40 individual HYSCORE data matrices were accumulated. Dataset–2 has a high resolution and a high SNR. Dataset 3: 200×200 points, time increments of $\Delta t = 16$ ns (Nyquist frequency 2×31.25 MHz, t_1, $t_2 = 3184$ ns), repetition time 0.7 ms. A total of 200 accumulations were recorded as 1 HYSCORE time-domain matrix with a total acquisition time of ca. 202 min. Dataset-3 has acceptable spectral resolution and a high SNR. The SNRs for these data sets were obtained by adjusting the number of acquisitions and reducing the sample concentration and sample position within the resonator to achieve the desired signal intensity.

Maximum entropy (MaxEnt) reconstructed spectra were computed using the Rowland NMR toolkit version 4 (http://rnmrtk.uchc.edu/rnmrtk/RNMRTK.html). The jittered exponential sampling algorithm incorporated in the program sched3d (version 5) [27] was used to generate the schedule for non-uniform sampling (NUS). The NUS scheme employed here for HYSCORE with two time-axes comprises a sparse matrix N_{rc} with an exponentially decaying density of points in both dimensions generated according to [4]

$$N_{rc} = R_{rc}^{1/\exp\left(-t_{1,c}/T_s\right)\exp(-t_{2,r}/T_s)}, \quad (5)$$

where time constant T_s is the same in each dimension for HYSCORE data, and R_{rc} is a random number, i.e. between 0 and 1. Only the (t_1, t_2) time points with N_{rc} values above a user set NUS cut-off value are kept. In this work the NUS level is given by variable *nus*, the fraction of (t_1, t_2) time points relative to the equivalent US scheme. For the combination of best sensitivity and resolution T_s is optimally adjusted in relation to the transverse relaxation times T^*_{2n} of the nuclear coherences ($T_s \sim 0.3 \times T^*_{2n}$) [8]. T^*_{2n} can be determined in a separate experiment measuring one long time trace of a HYSCORE experiment and determining from it when the ESEEMs decay to the noise level (e.g. inset in Fig. 7A). This trace serves to determine the time trace length required for maximum spectral resolution and can also be used to compute the noise level for setting an *aim* value for the MaxEnt algorithm (as discussed above).

MaxEnt reconstructions were performed in two dimensions using the program msa2d which requires the input parameters *aim* and *def*. During spectrum optimization λ is treated as an adjustable parameter and convergence is reached when $Q(\mathbf{d},\mathbf{f})$ is maximized and $C(\mathbf{f},\mathbf{d}) \leq aim$ (Eqs. (1) and (2)). The computation requires the number of points and the maximum frequency of the MaxEnt spectrum to be defined, which was set equal to that of the US data for ease of comparison to DFT spectra (the criteria for choosing the minimum time step in a NUS scheme is essentially the same as for the DFT method). Further details of how these parameters are set within the programs of the Rowland NMR toolkit are given in the Supporting Information. MaxEnt spectra were apodized with a Gaussian window function (convolution in the frequency domain) using a time constant consistent with the resolution governed by the maximum length of the experimental time traces unless otherwise stated (Fig. 6 is an exception).

3. Results

Our principal goal is to quantify and compare the sensitivity, resolution and linearity of HYSCORE spectra computed using US data with the DFT (US + DFT) to that of NUS data reconstructed with the MaxEnt algorithm (NUS + MaxEnt). Our analysis utilizes three HYSCORE data matrices with different signal-to-noise ratio (SNR) and spectral resolution (time trace lengths) all collected on a low-spin cytochrome P450 enzyme sample. These are referred to as dataset-1, dataset-2 and dataset-3 (see the Experimental section). Throughout *aim* and *def* are given relative to the noise level of the experimental data.

3.1. Sensitivity and resolution

To quantify the sensitivity and resolution of a HYSCORE experiment computed from the US + DFT and the NUS + MaxEnt methods data recorded with different numbers of accumulations (n_{acc}) and hence different SNRs are investigated. Accumulation refers to the number of signal acquisitions (averages) used to record a time-domain HYSCORE data matrix, $\mathbf{Y}(t_1,t_2)$. Constant measurement time and minimum measurement time experiments are characterised in the following.

Firstly, we quantify sensitivity and resolution of HYSCORE data recorded with a very low SNR and spectral resolution (dataset-1). This mimics the experimental conditions where sensitivity is a limiting factor as for example in a biological sample with low concentrations of paramagnetic centers. Dataset-1 has only sufficient signal to detect just one pair of cross-peaks with a SNR of $snr = 2.6$, 3.1 after summing $n_{acc} = 40$ accumulations of US data and using the DFT (Fig. 2A and Table 1). In this paper the SNR of a peak is computed as,

$$snr = I/(2.5 \times noise - rms), \quad (6)$$

where I is the mean of the signal intensity computed from the top 5% of points of a HYSCORE peak and *noise-rms* is the root-mean-square of a region of the spectrum where there is no signal. The denominator of $(2.5 \times noise\text{-}rms)$ in Eq. (6) is the approximate level at which peaks become discernable from noise. This level was carefully chosen by examination of HYSCORE contour plots. A $snr \leq 1$ thus indicates that no peak is detected.

Fig. 2B was computed using the same US + DFT method as in Fig. 2A but with HYSCORE data having only $n_{acc} = 4$ accumulations and there are now no cross-peaks definitively detected in the spectrum. The SNR of the two cross-peaks is estimated as $snr = 0.9$, 1.0 (Table 1). For this calculation the peak intensities are estimated by scaling the corresponding peak intensity from the $n_{acc} = 40$ accumulation data where they are well defined. To investigate sensitivity using the NUS + MaxEnt methodology the total experiment time was kept constant to that used for the $n_{acc} = 4$ data and NUS data was constructed using fewer points but more averages per

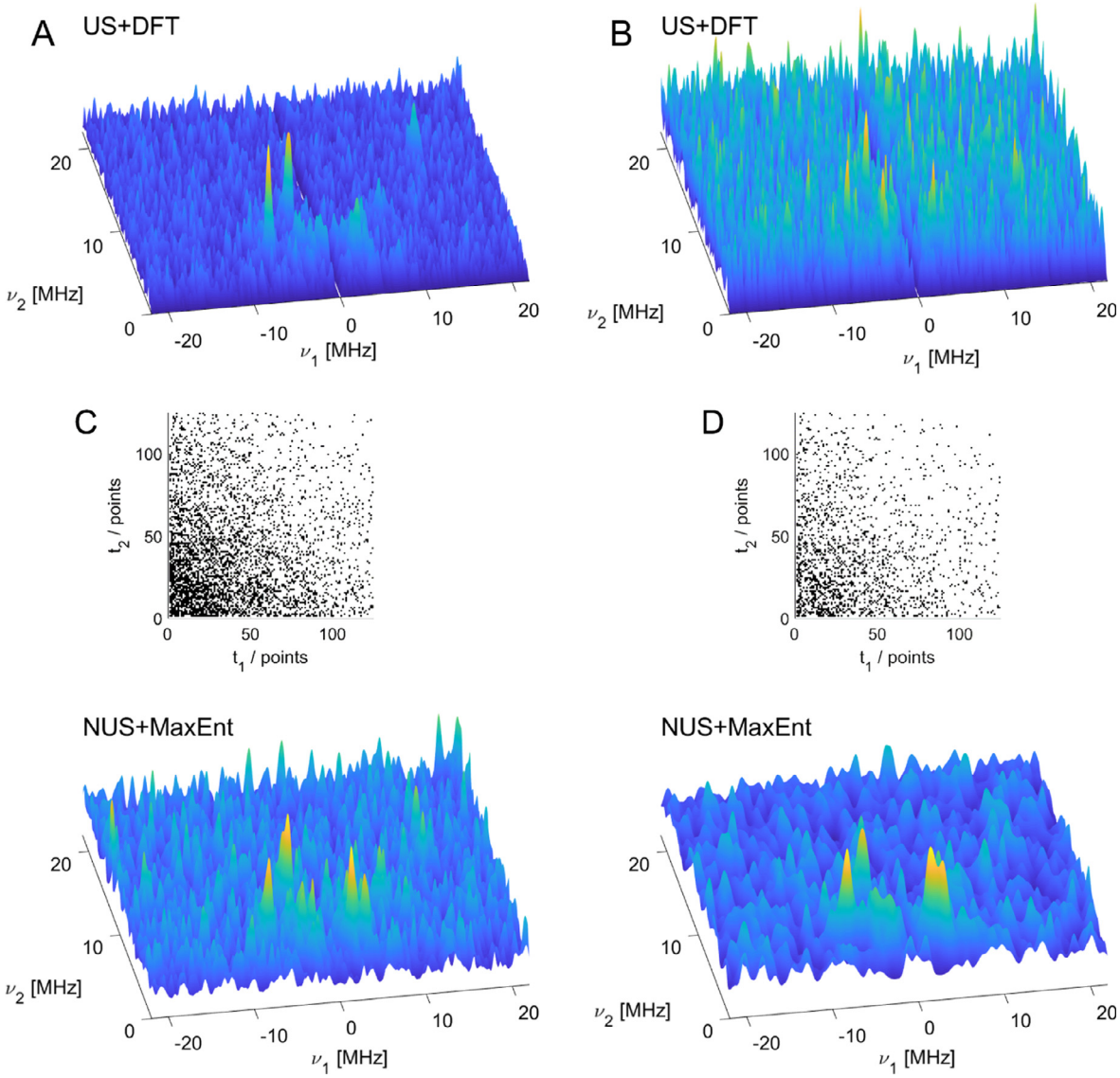

Fig. 2. HYSCORE spectra for dataset-1 computed with US + DFT and with NUS + MaxEnt for different number of accumulations (n_{acc}). (A) DFT spectrum, $n_{acc} = 40$, maximum SNR. Constant time experiments: (B) DFT spectrum, $n_{acc} = 4$; (C) MaxEnt spectrum with *nus* = 0.2, $n_{acc} = 20$, *aim* = 0.5, *def* = 0.01; (D) MaxEnt spectrum with *nus* = 0.1, $n_{acc} = 40$, *aim* = 0.5, *def* = 0.01. Inset in (C) and (D) shows the density of points for the random exponential NUS scheme with $T_s = 1.020$ μs in Eq. (5) (t_1, $t_2 = 2.480$ μs).

Table 1
Sensitivity parameters for dataset-1 (t_1, t_2 = 2.480 μs) using US + DFT and NUS + MaxEnt methodologies. Compared are HYSCORE data acquired with 'Constant Measurement Time', and 'Minimum Measurement Time to Detect Peaks'. *snr* and s^{ME} values are for the two weak cross-peaks detected using the US + DFT and NUS + MaxEnt methods, respectively. NUS(T_s μs) indicates the sampling density time constant in Eq. (5) and $T^*_{2n} \sim 6$ μs. Parameters *aim* and *def* are given relative to the noise level.

Methodology	Points	n_{acc}	Relative Total Time	*snr*	s^{ME}	*aim*	*def*
US	125 × 125	40	10	2.6,3.1	–	–	–
Constant measurement time							
US	125 × 125	4	1	0.9, 1.0	–	–	–
NUS(1.02 μs)[a]	20% (3125)	20	1	2.0, 2.3	3.3, 3.2	0.5	0.005
NUS(1.02 μs)[a]	10% (1562)	40	1	2.6,3.1	1.8, 3.0	0.5	0.005
Minimum measurement time to detect peaks							
US	125 × 125	6	1	1.4, 1.4	–	–	–
NUS(1.02 μs)[a]	20% (3125)	8	0.26	1.6,1.7	1.7, 1.6	0.5	0.005
NUS(1.02 μs)[a]	10% (1562)	10	0.17	1.8,2.1	2.4, 3.0	0.5	0.005

[a] T_s was set to a value less than $0.3 \times T^*_{2n} \sim 1.8$ μs which was found to increase sensitivity but with the loss of resolution (which is already limited with t_1, t_2 = 2.480 μs).

point. Two NUS levels were employed, [*nus* = 0.2, n_{acc} = 20], and [*nus* = 0.1, n_{acc} = 40], which give a sensitivity to detect peaks of s^{ME} = 3.3, 3.2 and s^{ME} = 1.8, 3.0, respectively, where s^{ME} is calculated using Eq. (6). Fig. 2C and D demonstrates graphically that the method is sufficient to detect the peaks at a high confidence level. Note that for all MaxEnt spectra the SNR is denoted s^{ME} to emphasize that it is not the intrinsic SNR of the raw data. s^{ME} may exceed the intrinsic SNR of the raw data substantially and furthermore it depends upon the user input parameters *aim* and *def* as discussed in detail below. At this stage we note that the ability to detect a peak (an $s^{ME} > 1$) is not critically dependent upon *aim* and *def* as long as they provide for an acceptable fit of the MaxEnt spectrum to the data. In this paper s^{ME} can be interpreted as indicating the statistical significance of detecting a peak.

Thus, increasing the SNR of points by increasing n_{acc} = 4 to n_{acc} = 20 (40) with a corresponding decrease in the number of points by 0.2 (0.1) increases the sensitivity to detect weak peaks with intensities close to the noise level. This result indicates a level of redundancy in the US HYSCORE data. Note that for the equivalent US data with n_{acc} = 20 (40) the cross-peaks in the DFT spectrum have a *snr* = 2.0, 2.3 (2.6, 3.1) demonstrating that the intrinsic SNR is in principle sufficient to detect the cross-peaks (Table 1). This analysis establishes that for a *constant time experiment* best sensitivity is obtained with the NUS + MaxEnt method.

Key in determining the sensitivity of the MaxEnt spectrum is the sampling scheme employed. The insets in Fig. 2C and D show the density of points for the NUS schemes. If a completely random sampling scheme is employed ($N_{cr} = R_{cr}$ in Eq. (5)), then for constant time experiments the MaxEnt spectrum in terms of sensitivity is very similar to the one computed by the DFT using US data (data not shown) [28,29]. With random exponential sampling [10], the best sensitivity is obtained by setting T_s in Eq. (5) relative to T^*_{2n}.

Lastly for dataset-1, the minimum experimental time required to detect the two prominent cross-peaks was determined for both the US + DFT and the NUS + MaxEnt methodologies. For US + DFT, n_{acc} = 6 is required to definitively identify these cross-peaks with a *snr* = 1.4, 1.4 (Fig. S2A). The corresponding accumulations to just resolve the two-cross peak for the NUS + MaxEnt method was determined as: [*nus* = 0.2 → n_{acc} = 8, s^{ME} = 1.7, 1.6] and [*nus* = 0.1 → n_{acc} = 10, s^{ME} = 2.4, 3.0] (Fig. S2B/C). This indicates that the maximum time saving to record a spectrum where the two prominent cross-peaks are just detected is 0.26 (*nus* = 0.2) and 0.17 (*nus* = 0.1). A summary of the sensitivity parameters for dataset-1 is given in Table 1.

Because of the non-linearity of the MaxEnt reconstruction with weaker peaks attenuated relative to stronger ones, it is not straightforward to scale these results easily (in a linear manner) for HYSCORE data with an arbitrary accumulation n_{acc} to estimate MaxEnt sensitivity. However, the analysis above establishes a guideline for the sensitivity improvements when the signal-to-noise-ratio of the entire spectrum is close to the noise level – an important case where efforts to improve peak detection are key.

The above analysis on dataset-1 was carried out on information poor data where only two HYSCORE cross-peaks are definitively detected. In contrast dataset-2 contains a large number of detected peaks and ridges above the noise level which have a large signal intensity variation with a range of 50.2 (largest/smallest peak intensity). The DFT spectrum of dataset-2 determined from US data (400 × 400 points) measured with the best SNR experimentally available, n_{acc} = 40 accumulations, is shown in Fig. 3A. Dataset-2 also has a high spectral resolution with the time trace length (t_1, t_2 = 7.182 μs) being significantly longer than dataset-1 (t_1, t_2 = 2.480 μs) and just long enough for peak widths in the HSYCORE spectrum to be governed by the intrinsic nuclear transverse relaxation times T^*_{2N}. This was ascertained by shortening the Gaussian apodization window time constant methodically and observing where peaks start to broaden.

The same type of analysis as for dataset-1 was carried out on dataset-2, concentrating however on the sensitivity of the methodology to detect the weakest peaks in the presence of many significantly stronger ones. These weakest peaks are ≈1/50 of the maximum peak intensity of the HYSCORE spectrum and are due to (^{1}H, ^{14}N) and (^{14}N, ^{14}N) combination peaks and are marked in Fig. 3A as p1 to p3 (peak assignments are given in Fig. S1). With the US + DFT method and n_{acc} = 4, these weak peaks are not observed in the HYSCORE spectra (Fig. 3B) and are well below the detection limit with predicted SNRs of *snr* = 0.8–1.1 (see Table 2). As for dataset-1, these peaks are easily detected in NUS + MaxEnt spectra of the same overall measurement time but recorded with (*nus* = 0.2, n_{acc} = 20), and (*nus* = 0.1, n_{acc} = 40) as shown in Fig. 3C/D. The intrinsic data *snr* and s^{ME} of the peaks p1 to p3 for these cases are listed in Table 2, along with the *aim* and *def* values. Lastly, the minimum number of accumulations required to just detect the weak combination peaks p1–p3 was determined for the US + DFT spectrum and the NUS + MaxEnt spectra at 20% and 10% of the points of the US data matrix; for US + DFT → n_{acc} = 7 accumulations; *nus* = 0.2 → n_{acc} = 9 accumulations per point; *nus* = 0.1 → n_{acc} = 13 accumulations per point. This represents a time saving of 0.25 and 0.19 for *nus* = 0.2 and *nus* = 0.1, respectively.

To match the experimental time of the best NUS + MaxEnt spectrum with *nus* = 0.1, the US HYSCORE data matrix could be reduced to 172 × 172 points. This then yields a spectrum with sensitivity comparable to the NUS + MaxEnt case but with a very significant loss of spectral resolution with peaks significantly broadened (Fig. S3). Dataset-2 thus demonstrates that very high resolution HYSCORE spectra can be recorded in a significantly faster time than the equivalent high resolution US + DFT spectrum.

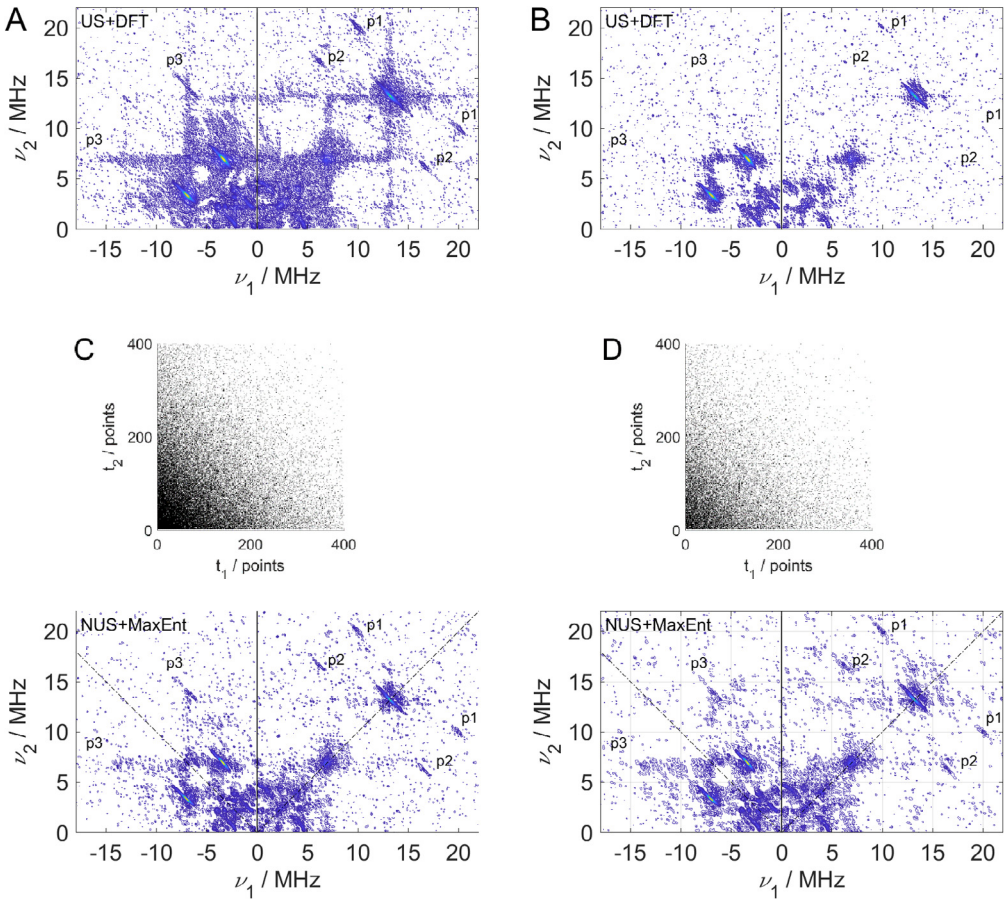

Fig. 3. HYSCORE spectra for dataset-2 computed with US + DFT and with NUS + MaxEnt for different numbers of accumulations (n_{acc}). The contour level cutoff was set to ~2.5 × noise-rms for spectra B, C and D. (A) DFT spectrum, n_{acc} = 40, maximum SNR. Constant time experiments: (B) DFT spectrum, n_{acc} = 4; (C) MaxEnt Spectrum with n_{acc} = 20, *nus* = 0.2, *aim* = 0.5, *def* = 0.01; (D) MaxEnt spectrum with n_{acc} = 40, *nus* = 0.1, *aim* = 0.5, *def* = 0.01. Inset in (C) and (D) shows the density of points for the random exponential NUS scheme with T_s = 1.800 μs in Eq. (5) (t_1, t_2 = 7.182 μs).

Table 2
Sensitivity parameters for dataset-2 (t_1, t_2 = 7.182 μs) using US + DFT and NUS + MaxEnt methodologies. Compared are HYSCORE data acquired with 'Constant Measurement Time' and 'Minimum Measurement Time to Detect Peaks'. *snr* and s^{ME} values are given for the six weakest cross-peaks p1 to p3 using the US + DFT and NUS + MaxEnt methods, respectively. NUS(T_s μs) indicates the sampling density time constant in Eq. (5) and $T^*_{2n} \sim 6$ μs. Parameters *aim* and *def* are given relative to the noise level.

Methodology	Points	n_{acc}	Relative Total Time	*snr* peaks p1 to p3	s^{ME} peaks p1 to p3	*aim*	*def*
US	400 × 400	40	10	1.7/1.3, 2.3/2.2, 2.5/2.1	–		
Constant measurement time							
US	400 × 400	4	1	0.9/0.8, 1.0/0.9, 1.1/1.0	–		
NUS(1.8 μs)	20%[a]	20	1	1.3/1.1, 1.6/1.7, 1.9/1.7	3.9/2.6, 4.9/4.9, 5.3/5.5	0.5	0.01
NUS(7.9 μs)	20%[a]	20	1	" "	1.5/1.2, 1.6/1.8, 1.9/1.7	0.5	0.01
NUS(1.8 μs)	10%[b]	40	1	1.7/1.3, 2.3/2.2, 2.5/2.1	5.2/3.9, 6.9/7.2, 7.5/8.0	0.5	0.01
NUS(7.9 μs)	10%[b]	40	1	" "	1.5/1.6, 4.7/1.6, 1.0/2.6	0.5	0.01
Minimum measurement time to detect peaks							
US	400 × 400	7	1	1/0.9, 1.1/1.1, 1.3/1.1	–	–	–
NUS(1.8 μs)	20%[a]	9	0.25	1/0.9, 1.2/1.2, 1.4/1.3	2.1/1.8, 3.2/3.2, 3.6/3.9	0.5	0.01
NUS(1.8 μs)	10%[b]	13	0.19	1.3/1.1, 1.6/1.7, 1.9/1.7	2.3/1.5, 2.8/2.6, 3.2/3.3	0.5	0.01

[a] 20% of 400 × 400 points is 32,000 points.
[b] 10% of 400 × 400 points is 16,000 points.

The analysis above for dataset-1 and dataset-2 concentrated on sensitivity to detect peaks, and thus on defining the frequencies measured in a HYSCORE experiment. Typically, this is the most important information available and simulation of the HYSCORE frequencies enables the magnetic parameters to be extracted. Theoretically the intensities (determined by coupling and relative orientation of the g-matrix, hyperfine matrix, etc) contain information on the interaction matrices and ideally should be matched by simulation to improve accuracy and solution uniqueness. However, approximations in the simulation generally make this information difficult to utilize (e.g. a simplified two- or three-spin system is simulated, relaxation is not included, square pulses are assumed) but nevertheless the linearity of the transformation is investigated in the following.

3.2. Linearity and sensitivity of the transformation on aim and def

An ideal property of the transformation of time domain data into the frequency domain is linearity of the transformation. Whilst this is guaranteed with the discrete Fourier transformation,

the linearity of a Maximum Entropy reconstruction depends upon the choice of the algorithm parameters *aim* and *def*. To investigate the effect of *aim* and *def* on the linearity of the transformation, and additionally the sensitivity, MaxEnt spectra were computed for a wide range of *aim* and *def* combinations: *aim* = 1, 0.5, 0.1, 0.01, 0.001 and *def* = 100, 10, 1, 0.1, 0.01, 0.001. For this analysis dataset-2 with high resolution is utilized and additionally the time-domain data were augmented with synthetic Lorentzian peaks with known amplitudes A and frequency positions (ν_1, ν_2),

$$L(t_1, t_2) = A \times \exp(-t_1/T - t_2/T)\cos(2\pi\nu_1 t_1 + 2\pi\nu_2 t_2) \quad (7)$$

The aim of the synthetic peaks is to determine if it is possible to quantify and potentially correct the non-linearity of a MaxEnt spectrum for a particular *aim* and *def*. In our protocol ten Lorentzian peaks were added to the time domain data with amplitudes evenly spaced from the most intense experimental peak to the data noise level and time constant T = 2.0 μs (t_1/t_2 = 7.182 μs). This type of synthetic peak method has been applied to NMR data in order to ascertain the degree of non-linearity on the MaxEnt transformation [6,17].

The non-linearity was characterised by plotting DFT peak intensities against those obtained from MaxEnt as shown in Fig. 4A for a representative case with *aim* = 0.5 and *def* = 0.01. The experimental data points indicated by the 'o' comprise 31 peaks and regions of ridges which were chosen to cover the signal intensity range of the data. Synthetic peaks are indicated by the '+' and are joined by a dotted line as a guide for the eye. All intensities are determined as an average of the top 5% of points (intensities) over the defined spectral region of the peak. The non-linearity observed in the synthetic peaks follows the general trend of the experimental peaks, with smaller amplitudes attenuated more relative to stronger ones in the MaxEnt spectrum, as expected. However, experimental peaks do not follow a simple monotonic trend that would allow the MaxEnt spectrum to be simply scaled with a calibration curve to accurately recover signal intensity linearity. This is

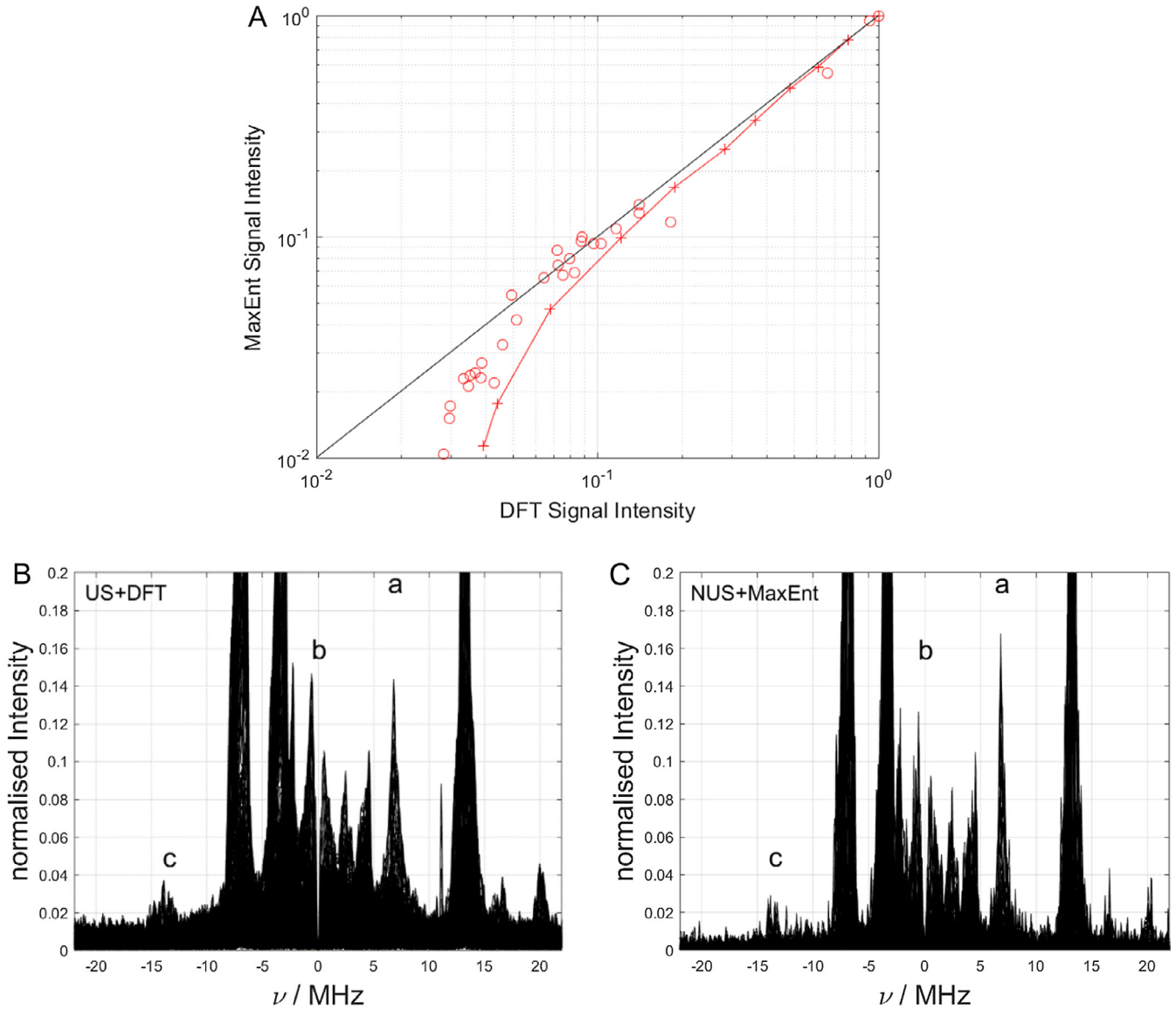

Fig. 4. Comparison of DFT and MaxEnt intensities for *aim* = 0.5 and *def* = 0.01 for dataset-2. (A) DFT vs MaxEnt peaks intensities. 'o' shows 31 experimental peak intensities which span the range of signal intensities in the data. Synthetic Lorentzian peaks are shown as '+' and are joined by a line as a guide to the eye. Both DFT and MaxEnt intensities are scaled so that the strongest peak has intensity 1. The data shows the typical trend for MaxEnt transformations where weaker peaks are increasingly attenuated relative to stronger ones. (B) and (C) show the projection of the DFT and MaxEnt HYSCORE spectra onto the ν_1 axis, respectively, for the data used to construct (A). The peak marked 'a' is larger in the MaxEnt spectrum, whereas 'b' and 'c' are larger in the DFT spectrum.

demonstrated in Fig. 4B/C which plots the data from which Fig. 4A was constructed as a projection of the 2D spectrum onto the ν_1 axis. Three peaks are highlighted; 'a' which is relatively stronger in the MaxEnt as compared to the DFT spectrum, and 'b' and 'c' where the corresponding peak is strongest in the DFT spectrum. Evidently, the NUS scheme introduces error or uncertainty in the intensities which cannot be faithfully recovered. Given this property the NUS + MaxEnt method is most useful in its ability to determine accurately spectrum frequencies, but some information on the exact intensities is lost. The addition of synthetic peaks allow the degree of non-linearity to be estimated but not accurately quantified.

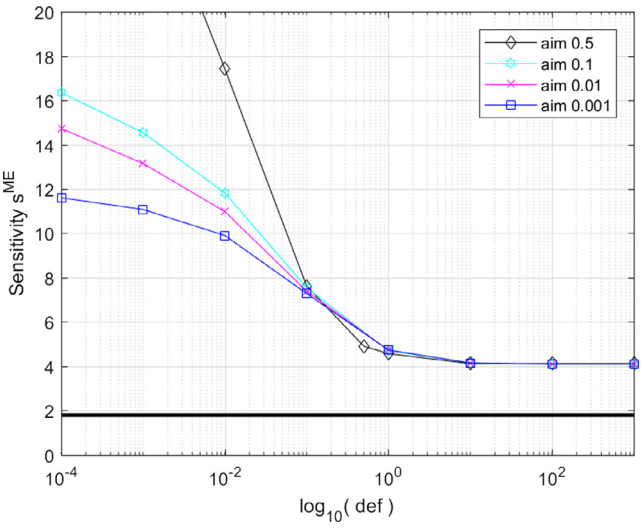

Fig. 5. Sensitivity of the NUS + MaxEnt method to detect the weakest HYSCORE peak in dataset-2 for a range of *aim* and *def* values. The black horizontal line shows the related intrinsic SNR of the corresponding US + DFT peak (n_{acc} = 20) as the MaxEnt data (*nus* = 0.2, n_{acc} = 20).

In addition to the non-linearity properties of the MaxEnt transformation it is instructive to investigate how sensitivity (to detect peaks) depends upon the choice of *def* and *aim*. For this purpose a weak peak in the spectrum of dataset-2 was chosen and s^{ME} plotted for a wide range of *aim* and *def* values, Fig. 5. The data show that s^{ME} is approximately constant when *def* > 1 for the range of *aim* values analyzed. With *def* < 1, s^{ME} increases rapidly with the best s^{ME} result having *aim* ~ 0.5 and the smallest *def*. The SNR of the corresponding US + DFT data with n_{acc} = 20 is shown as the black horizontal line. The data demonstrate that for HYSCORE a good choice for *aim* is in the range 0.5–0.1. Decreasing *def* < 1 increases the sensitivity or significance to detect weak peaks, but at the cost of increases in the non-linearity of the obtained spectrum [17]. This feature can be particularly disadvantageous when ridges with a large intensity variation are present in the spectrum as is typically the case for HYSCORE, as then the ridge itself can become quite distorted and potentially difficult to interpret. This is demonstrated in Fig. 6 for an extreme range of *def* values. In this figure the MaxEnt spectra were not apodized with a Gaussian window function to highlight the *def* dependence (Fig. S4 shows the corresponding data but with a window function applied with a time constant consistent with the resolution set by the time trace length).

3.3. Advantages of MaxEnt over the DFT for linearly sampled data

For linearly sampled data, an advantage of the MaxEnt transformation over the DFT is that there is no truncation of the time-domain data required; the MaxEnt spectrum is optimized in the frequency domain and only inverse Fourier transformed to the time-domain to compare to the experimental data during the optimization [30]. Thus MaxEnt does not suffer from time-domain truncation artifacts, 'sinc wiggles' or 'starred peaks'. Starred peaks resulting from the truncated time-domain traces can potentially overlap with weak real peaks and make data analysis inconclusive. This is shown in Fig. 7 for dataset-3 that has trace lengths t_1/t_2 = 3.148 μs. The DFT spectrum shown in Fig. 7A used a

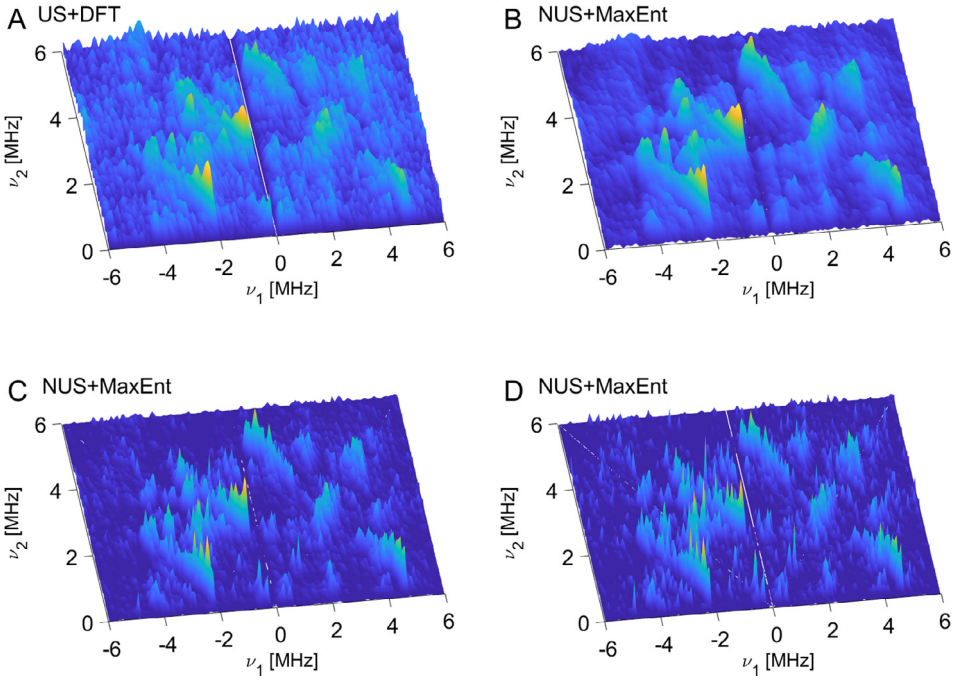

Fig. 6. HYSCORE spectra highlighting the distortion of the ridges as *def* is decreased for dataset-2 in the spectral region below 6 MHz. US + DFT spectrum (A) and NUS + MaxEnt spectra for *aim* = 0.5 with *def* = 0.5 (B), *def* = 0.01 (C), and *def* = 0.0001 (D). All spectra have the same measurements time: US + DFT → n_{acc} = 4; NUS + MaxEnt → *nus* = 0.2, n_{acc} = 20. No window function was used on the MaxEnt spectra.

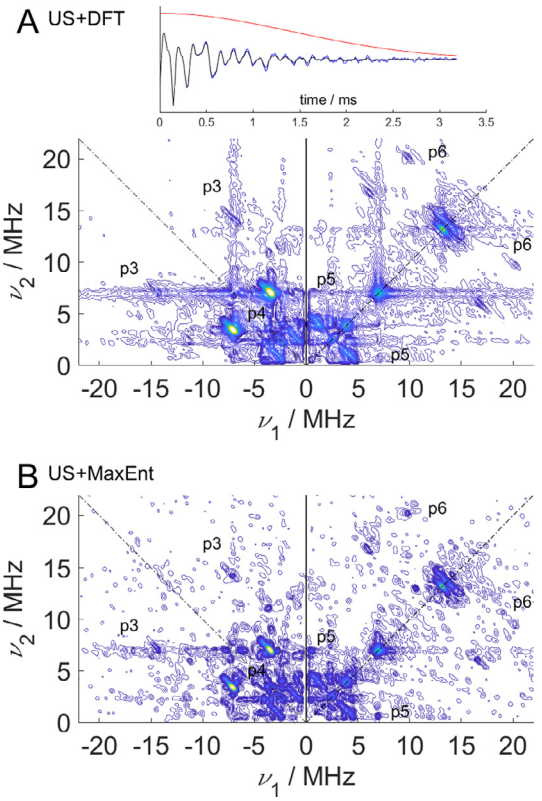

Fig. 7. HYSCORE spectra computed from dataset-3 all uniformly sampled. (A) US + DFT spectrum computed after application of a Gaussian window function with time constant T_{apz} = 2.000 μs (see inset). (B) US + MaxEnt spectrum with *aim* = 0.1 and *def* = 0.01. Starring ridges from the strongest peak which distorts weak peaks in the DFT spectrum are absent in the MaxEnt spectrum, see for example p3 to p5.

Gaussian window function with a time constant T_{apz} = 2.0 μs (see inset). The strongest cross-peaks at (−7, 4) MHz and (−4, 7) MHz exhibit starred ridges which overlap with a number of weak cross-peaks some of which are highlighted, see p3 to p5. The windowing artifacts are removed in the MaxEnt spectrum as shown in Fig. 7B computed with *aim* = 0.1 and *def* = 0.01. Peak p3 for example is detected at high significance with a s^{ME} = 3.9 and is now not distorted by a starred peak. In the MaxEnt spectrum some of the weakest peaks have an apparent lower *SNR* (detection sensitivity) than in the DFT spectrum, see for example peaks p6. This is dependent largely upon the exact choice of *aim* and *def*; with the current parameters these peaks are still detected and their shape reasonably preserved. Finally, the MaxEnt spectrum still exhibits an artefact ridge, now very weak, parallel to the ν_1 axis for $\nu_2 \sim 7$ MHz. This cannot be from a windowing artefact so must belong to an unwanted feature in the data itself (unknown but potentially caused by inaccuracies in removing the baseline).

4. Discussion

In this paper we compare and characterize how the methodologies of US + DFT and NUS + MaxEnt perform on a number of HYSCORE datasets with distinct properties. Firstly the sensitivity of the two methods were investigated on data where the signal intensity is at the limit to definitively detect just one pair of cross-peaks in the spectrum. This data (dataset-1) has a very poor SNR and short t_1/t_2 time traces, measurement conditions that may be encountered for example on biological samples with low concentrations of paramagnetic centers. For HYSCORE experiments with a constant measurement time it was shown that the NUS + MaxEnt method outperforms US + DFT by about a factor of 5. Importantly, for a constant time experiment where US + DFT was unable to detect the cross-peaks, MaxEnt was sensitive enough to detect these peaks.

In contrast to dataset-1, dataset-2 has many detected cross-peaks with a large range of signal intensities, with the weakest peaks close to the noise level. Dataset-2 has very long time traces such that the spectral resolution is close to the intrinsic linewidth set by spin system relaxation. Reductions in the NUS + MaxEnt measurement time as compared to the US + DFT measurement time by about a factor of 5 were again observed with an optimal choice of the sampling time T_s in the NUS scheme (Eq. (5)), i.e. $T_s \approx 0.3 \times T^*_{2n}$. This relationship is consistent with results from NMR studies [8]. The sampling scheme is key in determining the maximum sensitivity that can be obtained. If uniform weighting is employed in the NUS scheme (i.e. $N_{cr} = R_{cr}$ in Eq. (5)), there is no sensitivity advantage in the NUS + MaxEnt method as compared to the US + DFT method for a constant-time experiment (but there may be a resolution enhancement).

We characterized the non-linearity (Fig. 4) and sensitivity (Fig. 5) of MaxEnt spectra for a range of the user input parameters *aim* and *def*. Results show that *aim* and *def* should be at or below the noise level of the spectrum. A similar trend was observed in all HYSCORE data investigated, we thus suggest that a suitable, wide general range has *aim* = 1–0.1, and *def* = 1–0.001. Significantly smaller *def* values result in very large attenuations of the weakest signals. In the extreme case of very low *def,* severe distortion of HYSCORE ridge intensities may result because these intensities can vary strongly across a ridge and the significant MaxEnt intensity dependent attenuation makes the data difficult to interpret as a ridge may be broken into segments (Fig. 6). Results indicate that satisfactory HYSCORE spectra with acceptable ridge shape using NUS + MaxEnt can in general be obtained by searching in the range *aim* = 0.5–0.1 and *def* = 0.1–0.01.

Within the NMR literature there are three major regimes of choosing *aim* (or λ) and *def*: automated maximum entropy reconstruction (AUTO) [25], maximum entropy interpolation (MINT) [13], and Shannon-weighted augmentation of reconstruction (SHARP) [31]. AUTO uses *aim* set to the experimental noise level and the scaling factor *def* is based on *aim* and the number of dataset points, for HYSCORE $def = aim \times \sqrt{(M/N)} = aim$ as $M = N$ (equal number of rows and columns in a time-domain matrix). *MINT* [13] was introduced by Paramasivam and co-workers where the main strategy is to set *aim* lower than the noise level, and then *def* = *aim.* This can leads to overfitting of the solution for extremely low *aim* values. In SHARP [31] the approach is similar to AUTO, with *aim* set at the noise level but $def = aim/10^3$. We investigated these regions in our analysis. For HYSCORE applications we suggest operating in the region *aim* = 0.5–0.1 and *def* = 1–0.01, the approximate space covered by AUTO and SHARP. The lower *def* in SHARP gives higher sensitivity but tends to distort HYSCORE ridge intensities because of the larger non-linearity, AUTO has a larger *def* and thus better linearity is obtained in the MaxEnt spectrum.

Recently Zambrello and co-workers introduced an automated procedure to determine the optimum MaxEnt parameters (NUS scheme, *aim* and *def* values) for computation of spectra for solution-state NMR data containing many peaks. The method, in situ/receiver operating characteristic (IROC), is based on an in situ analysis of synthetic peaks introduced to an NMR spectrum. IROC uses two main metrics, recovery rate and false discovery rate, which are calculated as a function of the detection threshold, resulting in an IROC curve. The recovery rate is the fraction of synthetic peaks that are recovered, and the false discovery rate is the fraction of total peaks that are false positive (signal falsely identified as a peak). The detection threshold is set to a fraction of the estimated

spectrum noise. In this paper we considered sensitivity to detect peaks as a function of *aim*, *def* and the level of NUS, only introducing synthetic peaks to investigate non-linearity. For optimization of MaxEnt HYSCORE spectra we suggest computations within the suggested *aim* and *def* ranges (*aim* = 0.5–0.1 and *def* = 0.1–0.01) and a careful examination of spectra with an emphasis on the identification of cross-peaks to ensure only real peaks are identified. Given the relatively small number of peaks in a HYSCORE spectrum and the appearance of these peaks in characteristic regions of the spectrum, an automated peak detection procedure like IROC will generally not be required for HYSCORE data.

Because the HYSCORE spectrum has symmetry with respect to a pair of cross-peaks around the diagonals in both (+,+) (≡ (−,−)) and (−,+) (≡ (+,−)) quadrants, it is perhaps advantageous to use this property in the MaxEnt algorithm, i.e. symmetrize the time-domain data matrix, $Y^{symm} = ½(Y + Y^{\dagger})$ (where † indicates transpose), and then in the frequency domain only intensities of ½ of the spectrum in the (+,+) and (−,+) quadrants would need to be optimized. However, we did not pursue this approach as the appearance of a pair of cross-peaks enables confidence to assign them as real rather than noise. Removing this useful property will likely result in many wrong assignments (false negatives in the MaxEnt spectrum).

5. Conclusion

HYSCORE is a widely used high-resolution pulse EPR technique but has the disadvantage of long measure times due to the point-by-point data acquisition demanded by two indirect dimensions. Long measurement times are required to obtain data with long time traces and thus high spectral resolution (increasing with N^2 where N is the number of points in each dimension). The sensitivity of the NUS + MaxEnt method was characterized for HYSCORE data with a low SNR and short time traces, and for data recorded with a high SNR and spectral resolution (long time traces). In all cases NUS + MaxEnt outperforms the US + DFT method in terms of sensitivity and resolution, but with the disadvantage of losing linearity of the signal intensities in the transformation, the degree of which depends upon the user input parameters *aim* and *def*. The time saving and sensitivity enhancement depends critically on employing a weighted NUS scheme, and consequently for measurement of high-resolution spectra the NUS + MaxEnt method is most impressive and beneficial. MaxEnt may also find application to transform uniformly sampled HYSCORE data to the frequency-domain as unlike the DFT it does not transform truncated time-domain data which produces 'starred peaks' in the frequency-domain.

Current commercial EPR spectrometers are not configured optimally to support non-uniform sampling schemes that would greatly benefit multi-dimensional pulse EPR experiments with a number of indirect dimensions. Incorporating such a capability into existing spectrometers and in the design of new spectrometers we believe will open up many new exciting possibilities.

Acknowledgement

This work was supported by ARC Grant FT120100421 (J.R.H.), by a Centre for Advanced Imaging Ph.D. Scholarship (A.E.M.), and resources made available by the Centre for Advanced Imaging, The University of Queensland.

Appendix A. Supplementary material

Supplementary data to this article can be found online at https://doi.org/10.1016/j.jmr.2019.02.002.

References

[1] A. Schweiger, G. Jeschke, Principles of pulse electron paramagnetic resonance, 2001.
[2] S. Stoll, R.D. Britt, General and efficient simulation of pulse EPR spectra, Phys. Chem. Chem. Phys. 11 (2009) 6614–6625.
[3] P. Höfer, A. Grupp, H. Nebenführ, M. Mehring, Hyperfine sublevel correlation (hyscore) spectroscopy: a 2D ESR investigation of the squaric acid radical, Chem. Phys. Lett. 132 (1986) 279–282.
[4] K.K. Nakka, Y.A. Tesiram, I.M. Brereton, M. Mobli, J.R. Harmer, Non-uniform sampling in EPR–optimizing data acquisition for HYSCORE spectroscopy, Phys. Chem. Chem. Phys. 16 (2014) 16378–16382.
[5] G.L. Bretthorst, Nonuniform sampling: bandwidth and aliasing, Concepts Magn. Reson. Part A Bridg. Educ. Res. 32A (2008) 417–435.
[6] J.C. Hoch, A.S. Stern, Maximum entropy reconstruction, spectrum analysis and deconvolution in multidimensional nuclear magnetic resonance, Meth. Enzymol. 338 (2002) 159–178.
[7] K. Kazimierczuk, W. Kozminski, I. Zhukov, Two-dimensional Fourier transform of arbitrarily sampled NMR data sets, J. Magn. Reson. 179 (2006) 323–328.
[8] M. Mobli, J.C. Hoch, Maximum entropy spectral reconstruction of non-uniformly sampled data, Concepts Magn. Reson. Part A Bridg. Educ. Res. 32A (2008) 436–448.
[9] M.W. Maciejewski, H.Z. Qui, I. Rujan, M. Mobli, J.C. Hoch, Nonuniform sampling and spectral aliasing, J. Magn. Reson. 199 (2009) 88–93.
[10] M. Mobli, A.S. Stern, W. Bermel, G.F. King, J.C. Hoch, A non-uniformly sampled 4D HCC(CO)NH-TOCSY experiment processed using maximum entropy for rapid protein sidechain assignment, J. Magn. Reson. 204 (2010) 160–164.
[11] S.G. Hyberts, H. Arthanari, G. Wagner, Applications of non-uniform sampling and processing, Top. Curr. Chem. 316 (2012) 125–148.
[12] M. Mobli, M.W. Maciejewski, A.D. Schuyler, A.S. Stern, J.C. Hoch, Sparse sampling methods in multidimensional NMR, Phys. Chem. Chem. Phys. 14 (2012) 10835–10843.
[13] S. Paramasivam, C.L. Suiter, G. Hou, S. Sun, M. Palmer, J.C. Hoch, D. Rovnyak, T. Polenova, Enhanced sensitivity by nonuniform sampling enables multidimensional MAS NMR spectroscopy of protein assemblies, J. Phys. Chem. B 116 (2012) 7416–7427.
[14] M.W. Maciejewski, M. Mobli, A.D. Schuyler, A.S. Stern, J.C. Hoch, Data sampling in multidimensional NMR: fundamentals and strategies, Top. Curr. Chem. 316 (2012) 49–77.
[15] M. Mobli, J.C. Hoch, Nonuniform sampling and non-Fourier signal processing methods in multidimensional NMR, Prog. Nucl. Magn. Reson. Spectrosc. 83 (2014) 21–41.
[16] S.G. Hyberts, J.G. Heffron, N.G. Tarragona, K. Solanky, K.A. Edmonds, H. Luithardt, J. Fejzo, M. Chorev, H. Aktas, K. Colson, K.H. Falchuk, J.A. Halperin, G. Wagner, Ultrahigh-resolution 1H–13C HSQC spectra of metabolite mixtures using nonlinear sampling and forward maximum entropy reconstruction, J. Am. Chem. Soc. 129 (2007) 5108–5116.
[17] P. Schmieder, A.S. Stern, G. Wagner, J.C. Hoch, Quantification of maximum-entropy spectrum reconstructions, J. Magn. Reson. 125 (1997) 332–339.
[18] P.J. Hore, NMR data processing using the maximum entropy method, J. Magn. Reson. 62 (1985) 561–567.
[19] J.C. Hoch, Maximum entropy signal processing of two-dimensional NMR data, J. Magn. Reson. 64 (1985) 436–440.
[20] J.C. Hoch, A.S. Stern, D. Donoho, I.M. Johnstone, Maximum entropy reconstruction of complex (phase-sensitive) spectra, J. Magn. Reson. 86 (1990) 236–246.
[21] G.J. Daniell, P.J. Hore, Maximum entropy and NMR - A new approach, J. Magn. Reson. 84 (1989) 515–536.
[22] A.S. Stern, K.B. Li, J.C. Hoch, Modern spectrum analysis in multidimensional NMR spectroscopy: comparison of linear-prediction extrapolation and maximum-entropy reconstruction, J. Am. Chem. Soc. 124 (2002) 1982–1993.
[23] J.C. Hoch, A.S. Stern, NMR Data Processing, Wiley-Liss, New York, 1996.
[24] M. Mobli, M.W. Maciejewski, M.R. Gryk, J.C. Hoch, An automated tool for maximum entropy reconstruction of biomolecular NMR spectra, Nat. Methods 4 (2007) 467–468.
[25] M. Mobli, M.W. Maciejewski, M.R. Gryk, J.C. Hoch, Automatic maximum entropy spectral reconstruction in NMR, J. Biomol. NMR 39 (2007) 133–139.
[26] T.H. Edwards, S. Stoll, A Bayesian approach to quantifying uncertainty from experimental noise in DEER spectroscopy, J. Magn. Reson. 270 (2016) 87–97.
[27] M. Mobli, Reducing seed dependent variability of non-uniformly sampled multidimensional NMR data, J. Magn. Reson. 256 (2015) 60–69.
[28] D. Rovnyak, M. Sarcone, Z. Jiang, Sensitivity enhancement for maximally resolved two-dimensional NMR by nonuniform sampling, Magn. Reson. Chem. 49 (2011) 483–491.
[29] M.R. Palmer, B.R. Wenrich, P. Stahlfeld, D. Rovnyak, Performance tuning non-uniform sampling for sensitivity enhancement of signal-limited biological NMR, J. Biomol. NMR 58 (2014) 303–314.
[30] M. Mobli, A.S. Stern, J.C. Hoch, in: Fast NMR Data Acquisition: Beyond the Fourier Transform, Royal Society of Chemistry, London, England, 2017, pp. 252–266.
[31] T. Miljenovic, X. Jia, P. Lavrencic, B. Kobe, M. Mobli, A non-uniform sampling approach enables studies of dilute and unstable proteins, J. Biomol. NMR (2017).